Available online at www.sciencedirect.com
SCIENCE DIRECT®

Carbohydrate Polymers 63 (2006) 393–399

Carbohydrate Polymers

www.elsevier.com/locate/carbpol

High mechanical performance MMT-urea and formamide-plasticized thermoplastic cornstarch biodegradable nanocomposites

Mingfu Huang [a,b], Jiugao Yu [b,*], Xiaofei Ma [b]

[a] *Department of Chemical Engineering, School of Chemical Engineering and the Environment, Beijing Institute of Technology, Beijing 300072, China*
[b] *Department of Chemistry, School of Science, Tianjin University, Tianjin 300072, China*

Received 17 January 2005; received in revised form 3 September 2005; accepted 21 September 2005
Available online 2 November 2005

Abstract

Biodegradable nanocomposites have been successfully fabricated from the thermoplastic cornstarch (TPCS) and activated-montmorillonite (MMT) by melt-intercalation. TPCS was plasticized with novel plasticizers urea and formamide, and the activated-montmorillonites were obtained using citric acid as the activated solvent. Compared with urea and formamide-plasticized thermoplastic cornstarch (UFTPCS), the mechanical properties of nanocomposites were very good. The thermal analysis was investigated by Differential Scanning Calorimetry (DSC). The effect of water content on the mechanical properties of nanocomposites was studied. Dynamic Mechanical Thermal Analysis (DMTA) was also carried out. The structure and morphology of biodegradable nanocomposites were characterized by wide-angle X-ray diffraction (WAXD), scanning electron microscope (SEM) and transmission electron microscope (TEM). It was revealed that UFTPCS were intercalated into the layers of MMT successfully, and layers of MMT were fully exfoliated and so formed the exfoliated nanocomposites with MMT. This manufacturing process is simple and environmentally friendly.

Keywords: Biodegradable; Nanocomposites; Corn starch; Citric acid

1. Introduction

Since the methods of polymer intercalation and intercalative polymerization resolve the dispersion and interface problems in the preparation of polymer nanocomposites, the polymer/montmorillonite (MMT) nanocomposites have developed rapidly in the recent decade (Gross & Kalra, 2002; Lu, Yang, Sellinger, Lu, Huang and Fan, 2001; Merkel, Freeman, Spontak, He, Pinnau and Meakin, 2002; Okamoto, Nam, Maiti, Kotaka, Hasegawa and Usuki, 2001; Ray & Okamoto, 2004; Ray, Yamada, Okamoto, & Uede, 2002; Usuki, Hasegawa, Kadoura, & Okamoto, 2001). Currently, the matrixes of nanocomposites are mainly synthetic polymers, such as polyolefin, polyamide, polyester, and so on (Koerner, Jacobs, Tomlin, Busbee, & Vaia, 2004; Lee, Park, Yoon, & Kim, 2001; Osman, Atallah, 2004; Sun & Garces, 2002; Zilg, Thomann, Muhaupt, & Finter, 1999). However, studies on natural polymers are limited, and the material prepared from natural polymers has poor performance or a high cost. For example, thermoplastic starch/tunicin whiskers nanocomposites are expensive because of the high price of tunicin whiskers (Angles & Dufresne, 2000, 2001); Park et al. (Park, Lee, Park, Cho, & Ha, 2003; Park, Li, Jin, Park, Cho and Ha, 2002; Park, Misra, Drzal, & Mohanty, 2004) prepared the thermoplastic starch (TPS)/clay hybrids in which the weight ratio of native potato starch/water/glycerol contained in TPS was 5/2/3, and they studied the combination of natural polymers and inorganic mineral at the nanometer level, however, the mechanical properties of the hybrids were poor. The thermoplastic cornstarch (TPCS) plasticized by different plasticizers was prepared in our previous study, in which the crystallization behaviors of these materials resulting from longtime storage was inhibited, but the mechanical properties were still poor (Huang, Yu, & Ma, 2004; Ma & Yu, 2004a-c; Ma, Yu, & Feng, 2004).

Starch is attractive because it is a cheap material and has very fast biodegradability (Carvalho, Zambon, Curvelo, & Gandini, 2003). In order to obtain a biodegradable material with good mechanical properties, thermoplastic cornstarch plasticized by urea and formamide/citric acid-activated montmorillonite (UFTPCS/MMT) nanocomposites were

---

* Corresponding author. Tel./fax: +86 22 2740 6144.
E-mail address: mfhuang@21cn.com (J. Yu).

0144-8617/$ - see front matter © 2005 Published by Elsevier Ltd.
doi:10.1016/j.carbpol.2005.09.006

prepared by melt-intercalation in this study. The weight ratios of starch/urea/formamide were 10/2/1. It was discovered that the use of the novel plasticized system and the formation of the exfoliated nanostructure improved the mechanical properties of the biodegradable nanocomposites. The thermal properties and dynamic mechanical properties were investigated by DSC, DMTA, and the effect of water content on the mechanical properties of the nanocomposites was also studied.

2. Experimental

2.1. Materials

Cornstarch (11.5% moisture, 25% amylose) was obtained from Langfang Starch Company (Langfang, Heibei, China); Citric acid, formamide and ethanolamine were purchased from Tianjing Chemical Reagent Third Factory (Tianjin, China); Sodium montmorillonite (Na^+-MMT) with a cation exchange capacity (CEC) of 90–100 mmol/100 g as an inorganic host material was supplied by Zhangjiakou Qinghe Chemical Plant (Heibei, China).

2.2. Activation of MMT

About 5.04 g citric acid and 2.4 ml sulfuric acid (98%) were in turn added to 700 ml water at 80 °C. This solution was slowly added to a water solution that contained 20 g MMT. The mixture was stirred at 80 °C for 3 h, then cooled to room temperature, filtered and dried. After being ground and filtered, the citric acid-activated montmorillonite (CMMT) was obtained.

2.3. Preparation of biodegradable nanocomposites

The UFTPCS/MMT nanocomposites were prepared through two steps. For the first step, the urea (20 wt%) was dissolved with the formamide (10 wt%) to obtain the plasticizers (Ma & Yu, 2004; Ma et al., 2004), and the plasticizers were premixed (3000 rpm, 2 min) with cornstarch in the High Speed Mixer GH-100Y (made in China), and retained in the tightly sealed plastic bags for 48 h to swell the granular cornstarch molecules. Then these swollen mixtures were transferred into the single screw plastic extruder SJ-25 (s) (Screw Ratio $L/D = 25:1$, Beijing, China) with a screw speed of 20 rpm, so the UFTPCS was obtained. After processing, the UFTPCS were cooled and cut to small particles in order to be easily mixed with MMT powders. These UFTPCS granules were then mixed with different proportions of CMMT, and these mixtures were transferred to the single screw Plastic Extruder again. The extruder temperature profile of the first step and second step from feed zone to die was105, 110, 115, 120 °C (Ma et al., 2004). The die was a round sheet with 3 mm-diameter holes.

2.4. X-ray diffractometry

X-ray diffraction (XRD) analyses of the UFTPCS/CMMT nanocomposites, CMMT and MMT were carried out using a BDX3300 X-ray diffractometer (40 kV, 100 mA) equipped with a Ni-filtered Cu radiation and a curved graphite crystal monochromator. The scanning rate was 2°/min. The diffractometer was equipped with 1° divergence slit, a 0.16 mm receiving slit and a 1° scatter slit.

2.5. SEM and TEM

Scanning Electron Microscopy (SEM) morphologies were obtained using Philips XL-3. The samples were cooled in liquid nitrogen, and then fractured. The fracture faces were vacuum coated with gold for SEM. The nanocomposites specimens were performed with Transmission Electron Microscope (TEM) JEM-1200EX, operating at an acceleration voltage of 80 kV. The specimens were sliced in liquid nitrogen with the Reichert-Jung Ultracut E microtome, the thickness was 50–70 nm.

2.6. DSC testing

Differential Scanning Calorimetry (DSC) was performed with a NETZSCH DSC 204 equipment, fitted with a cooler system using liquid nitrogen. It was calibrated with an indium standard. Conditioned samples with 10 mg were placed in pressure-tight DSC cells, and at least three individual measurements were made to ensure reproducibility. Each sample was heated from −80 to 100 °C at a heating rate of 10 °C/min. The glass transition temperature (T_g) was taken as the inflection point of the specific heat increment at the glass–rubber transition.

2.7. Mechanical testing

According to the National Standard of China GB1040-79, the tensile stress and tensile strain of biodegradable nanocomposites were measured using Testometric AX M350-10KN Materials Testing Machines. The specimens were measured after being stored in a controlled chamber at RH50% for about 2 weeks. The crosshead speed was 10 mm/min. All measurements were performed for five specimens (80 mm × 3 mm in size) and averaged.

2.8. DMTA analysis

Dynamic mechanical thermal analysis (DMTA) was carried out with a NETZSCH DMA 242 instrument (Orientec Co.) in the tension mode with the following parameters: frequency = 3.33 Hz; scan rate = 3.0 K/min; temperature range = −100 to 100 °C. Samples (water content 11.5%) were prepared using the XX-I flat-sulfuration machine, and the dimension of sample was $16.0 \times 7.5 \times 2.5$ mm. The dynamic storage modulus (E'), loss modulus (E''), and mechanical loss tangent (tan $(=E''/E')$) were measured.

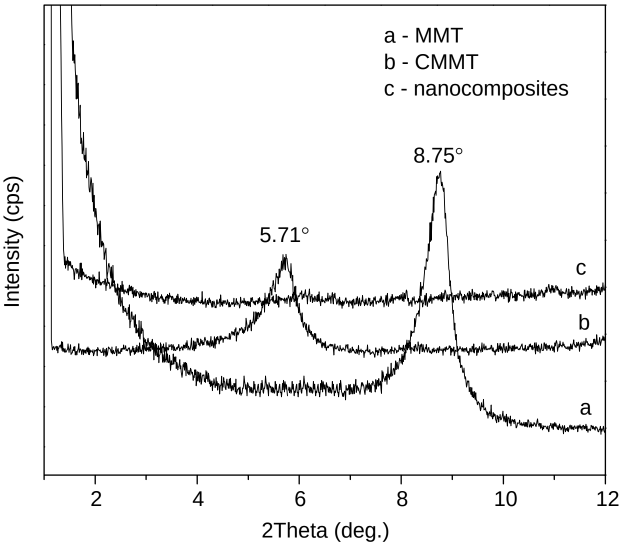

Fig. 1. XRD patterns of MMT, CMMT and UFTPCS/MMT nanocomposites.

3. Results and discussion

3.1. X-ray diffraction

The *X-ray diffraction* (XRD) patterns of MMT, CMMT and UFTPCS/MMT nanocomposites with 5 wt% CMMT were presented in Fig. 1.

As shown in Fig. 1, the diffraction peak of montmorillonite (001) crystal plane moved from 8.75 to 5.71°, when MMT was activated by citric acid. According to the Bragg diffraction equation, $2d \sin \theta = \lambda$, the spacing $d001$ between the layers are 1.01 and 1.55 nm, respectively, which indicated that the distances between the layers of MMT were widened, and the citric acid was intercalated into the layers of MMT. The microenvironment between the layers was ameliorated, which made MMT easy to react with UFTPCS. XRD pattern of nanocomposites showed that the diffraction peak $d001$ of nanocomposites disappeared. This indicated that the crystal lattice structure of MMT was totally dispersed, the slice layers were exfoliated into the UFTPCS, and combined with UFTPCS at the nanometer level, and so the exfoliated nanocomposites were formed.

3.2. Morphology

The SEM micrographs and the TEM images were presented in Fig. 2. As shown in the SEM micrographs of native cornstarch (Fig. 2a) and UFTPCS (Fig. 2b), the thermoplastic cornstarch plasticized by the urea and formamide formed a continuous UFTPCS phase, the cornstarch granules were destroyed, which was the foundation of preparing the nanocomposites with high performance. The SEM image (Fig. 2c) of nanocomposites with 5 wt% MMT showed that the MMT was uniformly dispersed in the UFTPCS. TEM micrograph of UFTPCS/MMT nanocomposites with 5% mass content MMT, which was magnified 100 thousand times, are presented in Fig. 2d. The white areas were UFTPCS phase

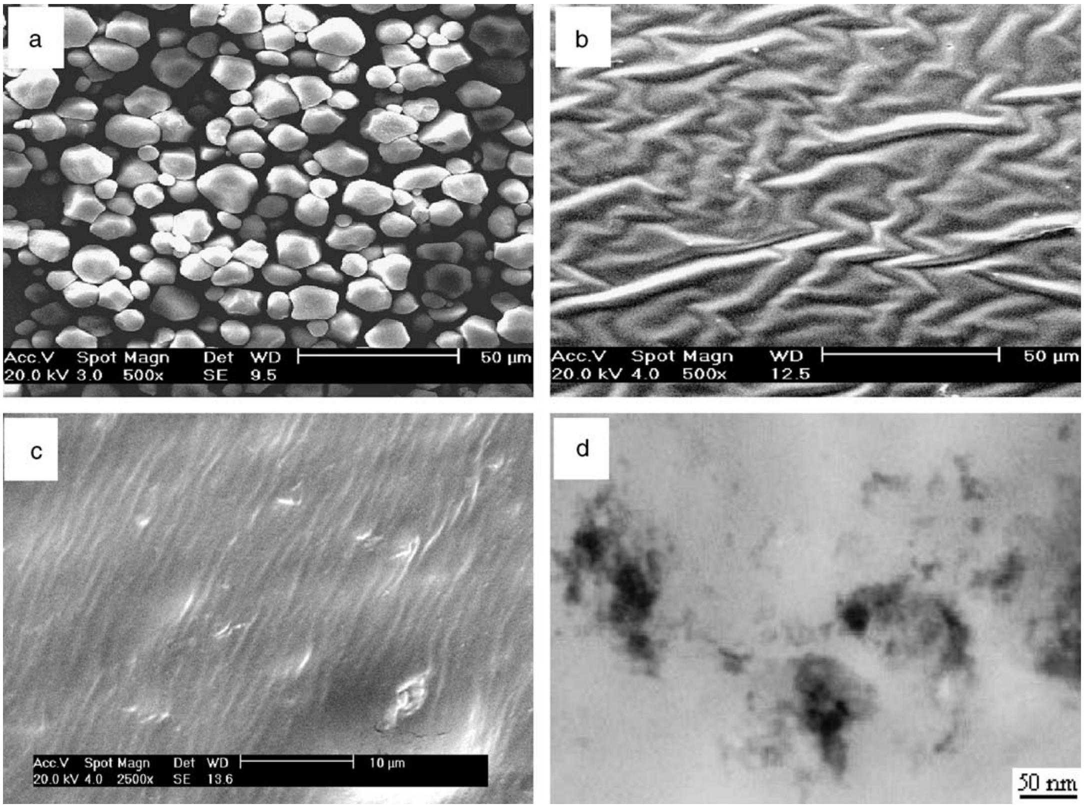

Fig. 2. Micrographs of different kinds of material. (a) SEM image of native cornstarch. (b) SEM image of UFTPCS. (c) SEM image of nanocomposites. (d) TEM image of nanocomposites.

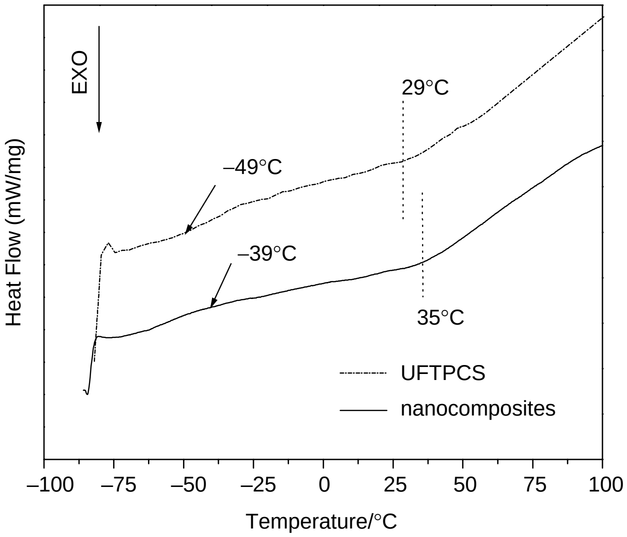

Fig. 3. DSC thermograms of nanocomposites with 5 wt% CMMT.

and the black areas were the exfoliated CMMT layers dispersed in UFTPCS phase. This indicated that a combination effect and thermal effect of single screw plastic extruder and the compatibility of MMT and UFTPCS, the melting UFTPCS molecular chains were intercalated in the MMT layers spacing successfully. The MMT layers were exfoliated (black areas) and uniformly dispersed in the UFTPCS matrix at nanometer level. The TEM results corresponded well with the WAXD patterns.

3.3. DSC analysis

Fig. 3 was the differential scanning calorimetry (DSC) traces of UFTPCS and biodegradable nanocomposites. Their DSC thermograms were quite similar, and both of them displayed two distinct ill-defined (as least for this heat capacity scale) specific heat increments. The low-temperature specific heat increment of the UFTPCS was located at −49 °C, and the high-temperature specific heat increment was located at 29 °C. The specific heat increments of the biodegradable nanocomposites were higher than that of the UFTPCS, which were located at −39 and 35 °C, respectively. The high-temperature specific heat increment reflected the glass transition temperature (T_g) of the biodegradable plastic using thermoplastic starch as the matrix, and the low-temperature specific heat increment indicated the movement of the smaller mobile unit, such as the short chains, side groups, some groups on the side groups, and branch chains in the starch molecular chain backbone, which was called the secondary transition. Lourdin, Bizot, and Colonna (1997) indicated that the low-temperature specific heat increment of thermoplastic starch (e.g. −49 and −39 °C) had little relation with the content of the plasticizer. The reason that the T_g and the secondary transition temperature of the biodegradable nanocomposites were higher than that of the UFTPCS was the MMT and the UFTPCS formed exfoliated nanostructure in nanocomposites, which restricted the molecular chain movement of UFTPCS.

3.4. Mechanical properties

3.4.1. The effect of MMT contents on the mechanical properties of biodegradable plastic

Fig. 4 showed that the tensile stresses of biodegradable nanocomposites with different MMT mass contents were obviously higher than that of UFTPCS. The tensile stress of biodegradable nanocomposites with 10 wt% MMT was the highest at 24.9 MPa. The biodegradable nanocomposites with

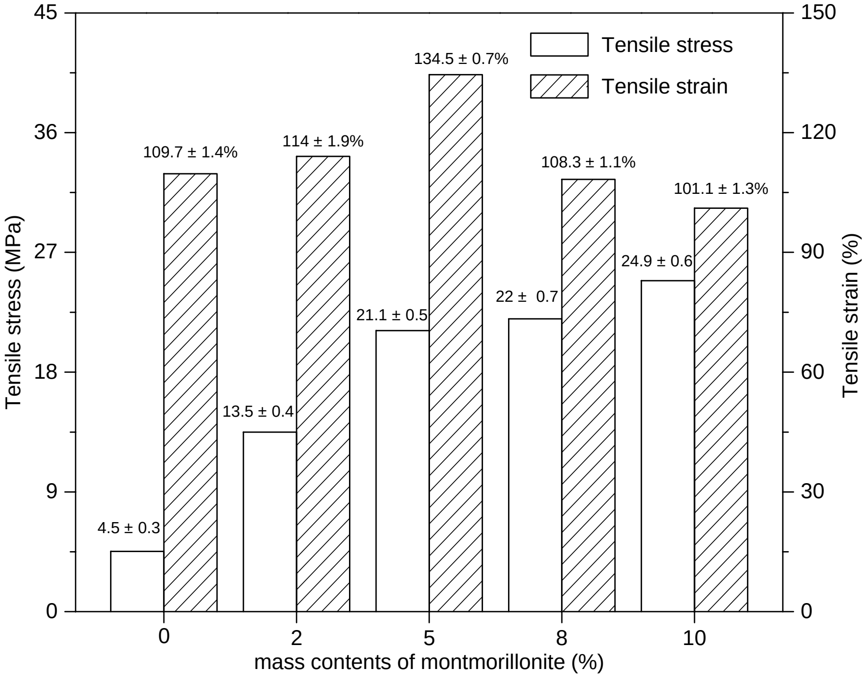

Fig. 4. The mechanical properties of UFTPCS and nanocomposites with different mass contents MMT.

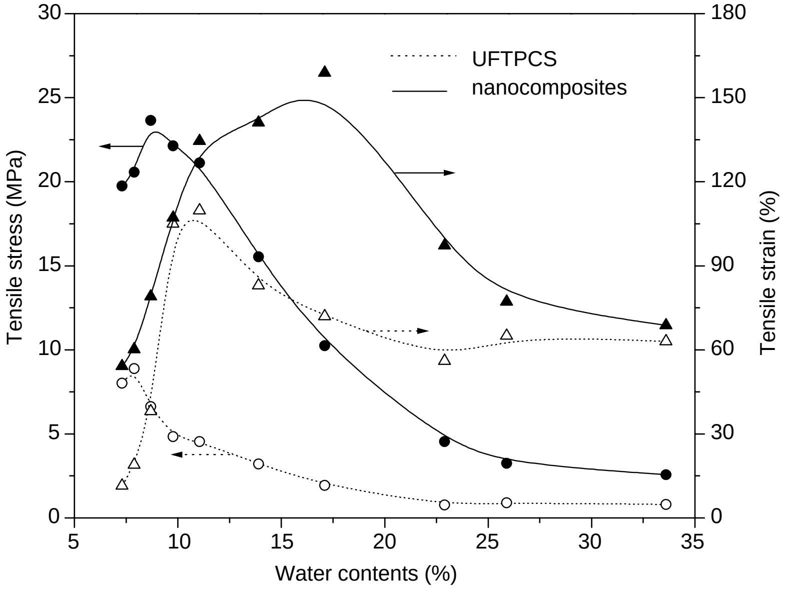

Fig. 5. The effect of water contents on the mechanical properties of UFTPCS and nanocomposites.

5 wt% MMT had the maximal tensile strain 134.5%. The mechanical properties of the biodegradable nanocomposites were very good, because the exfoliated MMT slices uniformly dispersed in the matrix of UFTPCS, and properly combined with the UFTPS on the interface, and so formed the stable polyphase nanostructure. The biodegradable nanocomposites with 5 wt% CMMT were worth further study because of their good mechanical properties.

3.4.2. The effect of water contents on the mechanical properties of biodegradable plastic

In general, the mechanical properties of biodegradable plastic using thermoplastic starch as the matrix were sensitive to the moisture content (Ma & Yu, 2004; Pamies, Roudaut, Dacremont, Le Meste, & Mitchell, 2000; Roudaut, Dacremont, & Le Meste, 1998; Roudaut et al., 1998), so the effect of the moisture content on mechanical properties of biodegradable nanocomposites and UFTPCS was studied here. Fig. 5 showed the effect of water contents on the biodegradable nanocomposites. With the increasing of water content (from 5 to 35%), the tensile stress and tensile strain first increased and then decreased. At low moisture content, the plastic became brittle presumably because of interaction between starch molecules. When the moisture content was high, the reaction between the starch molecules was weakened. Although the plastic became soft, both the tensile stress and the tensile strain decreased. In conclusion, the tensile stress and tensile strain of the biodegradable nanocomposites were higher than that of UFTPCS, which was caused by the strong interface reaction between the molecular chains of cornstarch and MMT in

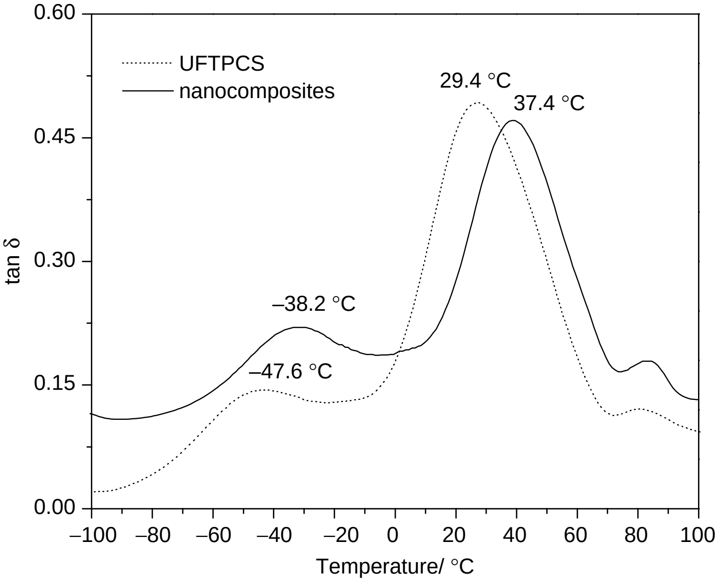

Fig. 6. The relation curves of tan (and the temperature of UFTPCS and nanocomposites.

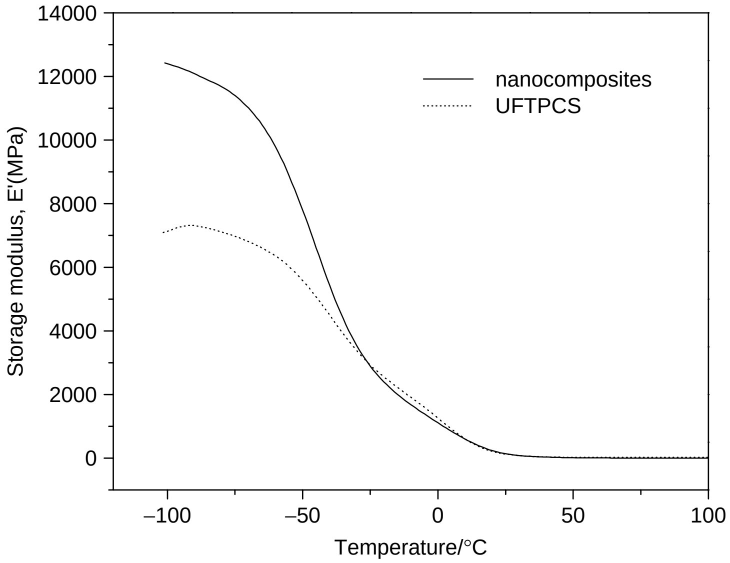

Fig. 7. Typical storage modulus behavior of UFTPCS and nanocomposites.

biodegradable nanocomposites. When the water content was 7.9%, the UFTPCS had the highest tensile stress at 8.9 MPa. When the water content was 11.05%, the UFTPCS had the highest tensile strain at 109.7%. For the biodegradable nanocomposites, they had preferable mechanical properties when the water content varied from 7.3 to 17.1%, and they had good ductibility when the water content varied from 9.8 to 22.9%. The maximal tensile stress of nanocomposites reached 23.7 MPa when the water content was 17.1%, and the highest tensile strain becomes 158.9% when the water content was 17.1%.

3.5. DMTA analysis

The dynamic storage modulus (E'), loss modulus (E''), and mechanical loss tangent ($\tan\delta = E''/E'$) with the change of temperature were measured by the Dynamic Mechanical Thermal Analysis (DMTA). E' was the storage and recovered energy. E'' represented energy in the form of heat in a cycle. The tan δ was ratio of loss to the storage energy in a cycle. Decreasing E' and the increasing tan δ indicated the elasticity of the material decreased, and the material was more easy to permanently deform. The inflections in E' and E'' temperature were accompanied by peaks in tan δ, which was the representation of material molecular transition, such as the glass transition temperature T_g, the transition point from the glassy to rubber state.

The T_g of dry corn starch was about 210 or 230 °C (derived from the extrapolated data), T_g of dry corn starch could not measured directly, (because it was very close to the decomposition temperature 225–250 °C) (Bikiaris and Panayiotou, 1998).

Figs. 6 and 7 showed the variation with temperature of the storage modulus and tan (for biodegradable plastic. According to the relation curves (Fig. 6) of tan (and the temperature, there were two transitions for the both plastics. The high-temperature transitions of UFTPCS and the nanocomposites were, respectively, 29.4 and 37.4 °C, the low-temperature transitions were −47.6 and −38.2 °C. The high-temperature transition of the biodegradable plastic was the glass transition. Compared with the T_g of dry starch, it was clearly defined. The T_g of UFTPCS (29.4 °C) was lower than that of nanocomposites (37.4 °C), because compared with UFTPCS, the starch molecular chain in nanocomposites was restricted by the MMT exfoliated nanostructure, and the degree of freedom decreased. It was important to note that the two transitions of biodegradable plastic measured by DMTA were basically in agreement with the two transitions measured by DSC (Roudaut, Dacremont, Pamies, Mitchell, & Le Meste, 2003; Roudaut et al., 2004).

In Fig. 7, the storage modulus of the two kinds of biodegradable plastic from −90 to 60 °C obviously decreased. The highest E' of biodegradable nanocomposites was close to 13,000 MPa that is 1.8 times than that of UFTPCS, which was all caused by the particular nanostructure of biodegradable nanocomposites.

4. Conclusion

Biodegradable nanocomposites were successfully obtained from the thermoplastic cornstarch (TPCS) and activated-montmorillonite by melt-intercalation. The thermoplastic cornstarch was plasticized with novel plasticizers urea and formamide and activated-montmorillonite were obtained using citric acid as the activated solvent. UFTPCS were intercalated into the layers of CMMT successfully; layers of MMT were fully exfoliated and formed the exfoliated nanocomposites with MMT, which were proved by Wide-angle X-ray diffraction (WAXD), scanning electron microscope (SEM) and transmission electron microscope (TEM). DSC analysis revealed that the specific heat increments of UFTPS were located at −49 and 29 °C, and those of biodegradable nanocomposites were located at −39 and 35 °C, which were basically accordant to the two transitions measured by DMTA. The mechanical properties of biodegradable nanocomposites were obviously better than that of UFTPCS. The biodegradable nanocomposites with 5 wt% MMT was a kind of biodegradable plastic with good mechanical stiffness and flexibility, and the maximal tensile strain reached 23.7 MPa when the water content was 8.7%, and the maximal tensile strain became 158.9% when the water content was 17.1%. The storage modulus of biodegradable nanocomposites was 1.8 times than that of UFTPCS. Those all had relations with the particular nanostructure of biodegradable nanocomposites. This manufacturing process was simple and environmentally friendly.

Acknowledgements

This work was supported by a grant from the PhD Programs Foundation of Ministry of Education of China (No. 200200556018).

References

Angles, M. N., & Dufresne, A. (2000). Plasticized starch/tunicin whiskers nanocomposites. *Macromolecules*, *33*, 8344–8353.

Angles, M. N., & Dufresne, A. (2001). Plasticized starch/tunicin whiskers nanocomposites. *Macromolecules*, *34*, 2921–2931.

Bikiaris, D., & Panayiotou, C. (1998). LDPE/starch blends compatibilized with PE-*g*-MA copolymers. *Journal of Applied Polymer Science*, *70*, 1503–1521.

Carvalho, A. J. F., Zambon, M. D., Curvelo, A. A. S., & Gandini, A. (2003). Size exclusion chromatography characterization of thermoplastic starch composites. *Polymer Degradation and Stability*, *79*, 133–138.

Gross, R. A., & Kalra, B. (2002). Biodegradable polymers for the environment. *Science*, *297*, 803–807.

Huang, M. F., Yu, J. G., & Ma, X. F. (2004). Studies on the properties of montmorillonite-reinforced thermoplastic starch composites. *Polymer*, *45*, 7017–7023.

Koerner, H., Jacobs, D., Tomlin, D. W., Busbee, J. D., & Vaia, R. D. (2004). Tuning polymer nanocomposite morphology: AC electric field manipulation of epoxy-montmorillonite suspensions. *Advanced Materials*, *16*, 297–302.

Lee, T. W., Park, O. O., Yoon, J., & Kim, J. J. (2001). Polymer-layered silicate nanocomposite light-emitting devices. *Advanced Materials*, *13*, 211–213.

Lourdin, D., Bizot, H., & Colonna, P. (1997). Antiplasticization in starch–glycerol films. *Journal of Applied Polymer Science*, *63*, 1047–1053.

Lu, Y. F., Yang, Y., Sellinger, A., Lu, M. C., Huang, J. M., Fan, H. Y., et al. (2001). Self-assembly of mesoscopically ordered chromatic polydiacetylene/silica nanocomposites. *Nature*, *410*, 913–917.

Ma, X. F., & Yu, J. G. (2004a). The plasticized containing amide groups for thermoplastic starch. *Carbohydrate Polymers*, *57*, 197–203.

Ma, X. F., & Yu, J. G. (2004b). Formamide as the plasticizer for thermoplastic starch. *Journal of Applied Polymer Science*, *93*, 1769–1773.

Ma, X. F., & Yu, J. G. (2004c). The effects of plasticizer containing amide groups on the properties of thermoplastic starch. *Starch*, *4*, 483–489.

Ma, X. F., Yu, J. G., & Feng, J. (2004). Urea and formamide as a mixed plasticizer for thermoplastic starch. *Polymer International*, *53*, 1780–1785.

Merkel, T. C., Freeman, B. D., Spontak, R. J., He, Z., Pinnau, I., Meakin, P., et al. (2002). Ultrapermeable reverse-selective nanocomposite membranes. *Science*, *296*, 519–522.

Okamoto, M., Nam, P. H., Maiti, P., Kotaka, T., Hasegawa, N., & Usuki, A. (2001). A house of cards structure in polypropylene/clay nanocomposites under elongational flow. *Nano Letters*, *1*, 295–298.

Osman, M. A., & Atallah, A. (2004). High-density polyethylene micro- and nanocomposites: Effect of particle shape, size and surface treatment on polymer crystallinity and gas permeability. *Macromolecular Rapid Communications*, *25*, 1540–1544.

Pamies, B. V., Roudaut, G., Dacremont, C., Le Meste, M., & Mitchell, J. R. (2000). Understanding the texture of low moisture cereal products: Mechanical and sensory measurements of crispness. *Journal of the Science of Food and Agriculture*, *80*, 1679–1685.

Park, H. M., Lee, W. K., Park, C. Y., Cho, W. J., & Ha, C. S. (2003). Environmentally friendly polymer hybrids. *Journal of Materials Science*, *38*, 909–915.

Park, H. M., Li, X. C., Jin, C. Z., Park, C. Y., Cho, W. J., & Ha, C. S. (2002). Preparation and properties of biodegradable thermoplastic starch/clay hybrids. *Macromolecular Materials and Engineering*, *287*, 553–558.

Park, H. M., Misra, M., Drzal, L. T., & Mohanty, A. K. (2004). Green nanocomposite from cellulose acetate bioplastic and clay: Effect of eco-friendly citrate plasticizer. *Biomacromolecules*, *5*, 2281–2288.

Ray, S. S., & Okamoto, M. (2004). Polymer/layered silicate nanocomposites: A review from preparation to processiong. *Progress in Polymer Science*, *28*, 1539–1641.

Ray, S. S., Yamada, K., Okamoto, M., & Uede, K. (2002). Polylactide-layered silicate nanocomposite: A novel biodegradable material. *Nano Letters*, *2*, 1093–1096.

Roudaut, G., Dacremont, C., & Le Meste, M. (1998). Influence of water on the crispness of cereal-based foods: Acoustic, mechanical, and sensory studies. *Journal of Texture Studies*, *29*, 199–213.

Roudaut, G., Dacremont, C., Pamies, B. V., Mitchell, J. R., & Le Meste, M. (2003). Rehydration of crispy cereal products: A tentative explanation of texture changes. *Freshness and Shelf Life of Foods ACS Symposium Series*, *836*, 223–234.

Roudaut, G., Poirier, F., Simatos, D., & Le Meste, M. (2004). Can dynamical mechanical measurements predict brittle fracture behaviour. *Rheologica Acta*, *44*, 104–111.

Roudaut, G., Van Dusschoten, D., Van As, H., Hemminga, M. A., & Le Meste, M. (1998). Mobility of lipids in low moisture bread as studied by NMR. *Journal of Cereal Science*, *28*, 147–155.

Sun, T., & Garces, J. M. (2002). High-performance polypropylene–clay nanocomposites by in-situ polymerization with metallocene/clay catalysts. *Advanced Materials*, *14*, 128–130.

Usuki, A., Hasegawa, N., Kadoura, H., & Okamoto, T. (2001). Three-dimensional observation of structure and morphology in nylon-6/clay nanocomposite. *Nano Letters*, *1*, 271–272.

Zilg, C., Thomann, R., Muhaupt, R., & Finter, J. (1999). Polyurethane nanocomposites containing laminated anisotropic nanoparticles derived from organophilic layered silicates. *Advanced Materials*, *11*, 49–52.